

Controlled Dephasing of a Quantum Dot: From Coherent to Sequential Tunneling

Daniel Rohrlich^{1,*}, Oren Zarchin^{1,†}, Moty Heiblum, Diana Mahalu, and Vladimir Umansky

*Braun Center for Submicron Research,
Department of Condensed Matter Physics,
Weizmann Institute of Science, Rehovot 76100 Israel*

(Dated: November 22, 2017)

Abstract

Resonant tunneling through identical potential barriers is a textbook problem in quantum mechanics. Its solution yields total transparency (100% tunneling) at discrete energies. This dramatic phenomenon results from coherent interference among many trajectories, and it is the basis of transport through periodic structures. Resonant tunneling of electrons is commonly seen in semiconducting “quantum dots”. Here we demonstrate that detecting (distinguishing) electron trajectories in a quantum dot (QD) renders the QD nearly insulating. We couple trajectories in the QD to a “detector” by employing edge channels in the integer quantum Hall regime. That is, we couple electrons tunneling through an inner channel to electrons in the neighboring outer, “detector” channel. A small bias applied to the detector channel suffices to dephase (quench) the resonant tunneling completely. We derive a formula for dephasing that agrees well with our data and implies that just a few electrons passing through the detector channel suffice to dephase the QD completely. This basic experiment shows how path detection in a QD induces a transition from delocalization (due to coherent tunneling) to localization (sequential tunneling).

*Current address: Department of Physics, Ben-Gurion University, Beersheva 84105 Israel.

†E-mail: oren.zarchin@weizmann.ac.il

¹Equal contribution

The study of entanglement began in 1935 with the EPR [1] and Schrödinger Cat [2] paradoxes, but it languished until Bell’s celebrated 1964 paper [3] and even thereafter. More recently, applications of entanglement to cryptography [4], “teleportation” [5], data compression [6] and computation [7] have given new impetus to the study of entanglement. Also the *loss* of interference (“decoherence” or “dephasing”) is studied, both as a condition for classical behavior to emerge from quantum systems and, more recently, as an obstacle to applications of entanglement. Here we report controlled partial and full dephasing of electron interference in a mesoscopic Fabry-Perot type interferometer—a quantum dot (QD)—entangled efficiently to a mesoscopic detector.

Mesoscopic interferometers [8] include closed [9] and open [10] two-path interferometers, QDs and double-QDs [11], and electronic Mach-Zehnder interferometers [12]. Mesoscopic detectors [8] include quantum point contacts (QPCs) [13, 14] and partitioned currents [11]. In our experiment, a QD serves as an interferometer of the Fabry-Perot type; the interference shows up as a resonant transmission peak in electron conductance through the dot. Figure 1 shows the QD. In order to couple tunneling and detector electrons strongly, we chose them from neighboring edge channels (i.e. in close proximity) in the integer quantum Hall regime. We worked at filling factors $\nu=2$ and $\nu=3$, but nothing in our results depends essentially on edge channels or a magnetic field. For the innermost quantum Hall edge channel (i.e. the channel farthest from the boundary) the dot is an interferometer. As electrons in the innermost channel tunnel through the dot, they become entangled with electrons passing freely through the neighboring, outer edge channel, which serves as a “detector” channel. These detector electrons couple coulombically to the total charge Q_{tun} tunneling through the dot, and their accumulated phase is proportional (via this Coulomb coupling) to the dwell time t_{dwell} of the tunneling electrons: $Q_{tun} = t_{dwell}I_{tun}$, where I_{tun} is the tunneling current. Detection broadens and quenches the resonance, consistent with the time-energy uncertainty principle: the decreased uncertainty in the dwell time entails increased uncertainty in the energy of the electrons.

According to a general principle [15], any determination of the path an electron takes through an interferometer, among all possible interfering paths, destroys the interference among the paths. Hence, coupling (entangling) a trajectory-sensitive detector and an electron interferometer should destroy the interference. In our experiment the detector is a partitioned channel current; it is partitioned at a quantum point contact (QPC) (not shown

in Fig. 1) before reaching the QD. Why partitioned? The detector current acquires a phase due to Coulomb coupling with the tunneling electrons in the inner channel. However, if the detector current is full (unpartitioned, noiseless) this phase is unobservable. Partitioning the detector current produces a transmitted *and* a reflected current; these two currents could interfere elsewhere and render the unobservable phase observable. Hence, partitioning the detector current allows us, in principle, to extract the additional phase due to coupling with electrons tunneling through the quantum dot. Now, whether or not we actually interfere the transmitted and reflected currents *elsewhere* cannot instantly produce any measurable change at the dot. Hence, a partitioned current must by itself dephase the electron resonance in the interferometer.

In this account, dephasing arises because the interfering quanta (electrons in the dot) leave “which path” information in the environment (detector current). Yet according to another general principle [16], there is always a complementary account: dephasing arises because the environment (detector current) produces fluctuating phases in the interfering quanta, and thus dephases the resonance. The partitioned current fluctuates: if N electrons arrive at a QPC that transmits with probability T , then NT are transmitted, on average, with typical fluctuations of $\sqrt{NT(1-T)}$. These fluctuations in the detector current (“shot noise” [17]) produce a fluctuating potential at the dot and thus a fluctuating phase in the tunneling electrons, which dephases the resonance.

For a Fabry-Perot interferometer, we can model the dephasing by calculating the effect of detection on interference. Let the first and second QPCs of the dot transmit with amplitudes t_1 and t_2 and reflect with amplitudes r_1 and r_2 , respectively. In the absence of a fluctuating phase, the amplitude t_{tun} for resonant transmission through the dot would be

$$t_{tun} = t_1 t_2 \left[e^{i\theta} + (r_1 r_2) e^{3i\theta} + (r_1 r_2)^2 e^{5i\theta} + \dots \right] = t_1 t_2 \sum_{j=0}^{\infty} (r_1 r_2)^j e^{i(2j+1)\theta} \quad ; \quad (1)$$

the sum includes an energy-dependent phase 2θ for each back-and-forth lap in the interferometer. However, we assume that during each back-and-forth lap, N electrons reach the QPC that partitions the detector current. Each transmitted detector electron induces an additional phase ϵ to a single back and forth trajectory of the resonant tunneling electron, while reflected detector electrons do not affect the tunneling electron. Indexing the detector electrons $k = 0, 1, 2, \dots$ according to their order of arrival at the detector QPC, we have additional phases ϵ_k where $\epsilon_k = \epsilon$ if the k -th electron is transmitted through the QPC and

$\epsilon_k = 0$ if it is reflected. Then for a given partitioning of the detector current we obtain not Eq. (1) but

$$t_{tun} = t_1 t_2 \sum_{j=0}^{\infty} (r_1 r_2)^j e^{i(2j+1)\theta} e^{i(\epsilon_0 + \epsilon_1 + \dots + \epsilon_{j \cdot N})} \quad . \quad (2)$$

Actually, Eq. (2) lacks the phase due to the first $N/2$ detector electrons to reach the detector QPC (i.e. as the tunneling electron first crosses the interferometer), but since this phase is common to all the terms in the sum, we neglect it. The transmission probability, given this partitioning, is the square of the absolute value of Eq. (2):

$$T_{tun} = |t_{tun}|^2 = T_1 T_2 \sum_{j, j'=0}^{\infty} (r_1 r_2)^j (r_1^* r_2^*)^{j'} e^{2(j-j')i\theta} e^{i \sum_{k=0}^{j \cdot N} \epsilon_k - i \sum_{k'=0}^{j' \cdot N} \epsilon_{k'}} \quad , \quad (3)$$

where $T_1 = |t_1|^2$, etc. We have to fold Eq. (3) with the probability distribution for the given partitioning of detector electrons. We do so in two steps. First, for a fixed $j - j' \geq 0$ in Eq. (3), we sum over j' ; that is, we consider

$$T_1 T_2 \sum_{j'=0}^{\infty} (r_1 r_2)^{j-j'} (R_1 R_2)^{j'} e^{2(j-j')i\theta} e^{i \sum_{k=j' \cdot N}^{j \cdot N} \epsilon_k} \quad . \quad (4)$$

We now fold the distribution of phases ϵ_k into Eq. (4) by replacing $e^{i \sum_{k=j' \cdot N}^{j \cdot N} \epsilon_k}$ with $(e^{i \cdot 0} R + e^{i \epsilon} T)^{(j-j')N}$, where R and T are, respectively, the probability for reflection and transmission of electrons from the detector QPC [18]. After summing over j' in Eq. (4), the next step is to sum over all values of $j - j'$. (Note that for $j - j' \leq 0$, we replace Eq. (4) by its complex conjugate.) The resulting transmission probability, which we denote $\langle T_{tun} \rangle$ to indicate the averaging over detector partitionings, is

$$\langle T_{tun} \rangle = \frac{T_1 T_2}{1 - R_1 R_2} \left[\frac{1}{1 - M} + \frac{1}{1 - M^*} - 1 \right] = \frac{T_1 T_2}{1 - R_1 R_2} \frac{1 - M^* M}{|1 - M|^2} \quad , \quad (5)$$

where $M \equiv e^{2i\theta} r_1 r_2 (R + e^{i\epsilon} T)^N$. The integral of $\langle T_{tun} \rangle$ over $\bar{\theta} \leq \theta \leq (\bar{\theta} + \pi)$, for any real $\bar{\theta}$, is independent of $|M|$ (as it must be since probabilities must sum to 1 for any strength of dephasing). For $R_{1,2} \gg T_{1,2}$ and small ϵ , Eq. (5) implies both broadening and quenching (decreased height) of the resonance peak in proportion to $NT(1 - T)$, as derived before [19]. Here, however, with the detector and tunneling currents so close, we cannot assume ϵ small.

The device, constructed from a GaAs-AlGaAs heterojunction (see Fig. 1), supported a high-mobility two-dimensional electron gas (2DEG). Biased metallic gates deposited on the surface of the heterojunction induced a controlled backscattering potential to form the quantum dot and quantum point contacts. The magnetic field was 5-7 Tesla, well within the

filling-factor 2 conductance plateau. Conductance was measured with a 0.9 MHz AC, 0.5 μV rms excitation voltage at an electron temperature of $\tau = 25$ mK. A low-noise cryogenic preamplifier in the vicinity of the sample amplified the measured voltage, followed by a room-temperature amplifier and a spectrum analyzer. An LC resonant circuit prior to the cold preamplifier allowed measurement of the signal at about 0.9 MHz with a bandwidth of about 100 Hz; see Ref. [20] for details.

Figure 2 shows dephasing of a series of Coulomb blockade peaks for various partitionings T of the detector current, at detector bias $V_D = 77\mu\text{V}$. For the horizontal axes we convert plunger gate potential to an effective dot potential (a “levering factor” extracted from Coulomb-diamond measurements [21]). The resonance peaks quench and broaden as T increases from 0 to 1/2 and reemerge as T increases from 1/2 to 1. At $T = 0$ there is no current in the detector to dephase the resonance. At $T = 1$ the resonance induces a constant phase in the electrons of the detector current, but the phase is not observable and there is again no dephasing. Only when T is between these limits does the detector current contain information about the resonance, and dephases it. Smaller detector bias implies less information in the detector current (or, in the complementary account, less shot noise in the detector current) hence less dephasing. Indeed, resonance peaks are less quenched at smaller detector bias.

Looking in detail at one conductance peak and fitting it with a Lorentzian curve, we obtain the width of the resonance peaks (Fig 2b). Undephased peaks have a full width at half maximum (FWHM) of about 12 μV , larger than $4k_B\tau \approx 9 \mu\text{V}$ (where k_B denotes the Boltzmann constant) at an estimated electron temperature of $\tau = 25$ mK. We found that T depended slightly on the detector bias. Thus, for each value of detector bias, we have calculated an effective transmission T_{eff} by averaging T with respect to energy, from the Fermi energy to the detector bias, and Fig. 3 shows dependence of (a) peak height and (b) peak width on T_{eff} , with the bias on the detector as an additional parameter.

To understand the relation between shot noise and dephasing quantitatively, let us define three times: t_{dwell} , t_{lap} and t_{det} . In the absence of temperature broadening, the dwell time t_{dwell} would be \hbar divided by 12 μV , the FWHM of the resonance. However, the FWHM is a convolution of coherent broadening and temperature broadening; only the former is relevant to the dwell time. Subtracting the temperature broadening $4k_B\tau \approx 9 \mu\text{V}$ from 12 μV we are left with 3 μV , so $t_{dwell} \approx \hbar/3\mu\text{V} \approx 220$ psec.

The dwell time is a multiple of the lap time, i.e. the time t_{lap} it takes an electron to go once back and forth in the dot. How many laps in a dwell time? To answer this question we return to Eq. (1) and note that a term $t_1 t_2 (r_1 r_2)^j e^{i(2j+1)\theta}$ in the series corresponds to $j + 1/2$ laps. Then the average number of laps made by an electron tunneling through the resonance is $\sum_j (j + 1/2) T_1 T_2 (R_1 R_2)^j$ divided by the total probability $\sum_j T_1 T_2 (R_1 R_2)^j$ to tunnel through the resonance, so it equals $1/2 + R_1 R_2 / (1 - R_1 R_2)$. In our experiment, we estimate $R_1 \approx R_2 \approx 2/3$ and so the average number of laps was approximately 1.3, i.e. the most likely path of an electron tunneling through the dot was to reflect twice inside the dot. Dividing t_{dwell} by the average number of laps, we obtain $t_{lap} \approx 170$ psec as the lap time. (From t_{lap} we can estimate the speed of an electron tunneling through the dot: if the effective inner length of the dot was roughly $0.25 \mu\text{m}$, then the electron traveled $0.5 \mu\text{m}$ in 170 psec, i.e. its speed was roughly $3 \cdot 10^5$ cm/sec, corresponding to a rather small electric field in the dot.)

Finally, the time t_{det} between successive electrons in the unpartitioned detector current I is $e/I = eR_H/V$ where R_H is the Hall resistance $R_H = h/e^2$ and V is the bias applied to the detector. Thus, $t_{det} = h/eV$, which was as low as 40 psec for the maximum detector bias of $103 \mu\text{V}$. For this maximum detector bias, an average of $N = 170$ psec/40 psec electrons, i.e. between 3 and 4 detector electrons reached the detector QPC during each lap of the tunneling electron; the number is proportionally smaller for smaller bias. This number corresponds to N above in Eqs. (2-5). Taking N to be proportional to the detector bias potential V , we find experimentally that the broadening and quenching of the resonance peak are both proportional to the shot noise $NT_{eff}(1 - T_{eff})$ at low detector bias ($10 \mu\text{V} \leq V \leq 50 \mu\text{V}$) but deviate from simple proportionality at larger bias (Fig. 3a). In particular, at larger bias, quenching of the resonance peak tends to saturate before T_{eff} reaches 0.5. This saturation is just what Eq. (5) implies, since the peak height (i.e. the difference between maximum and minimum values of $\langle T_{tun} \rangle$ as a function of θ) obtained from Eq. (5) is

$$\frac{T_1 T_2}{1 - R_1 R_2} \left[\frac{1 - Z}{(1 - \sqrt{Z})^2} - \frac{1 - Z}{(1 + \sqrt{Z})^2} \right] = \frac{T_1 T_2}{1 - R_1 R_2} \frac{4\sqrt{Z}}{1 - Z} \quad , \quad (6)$$

where $Z \equiv R_1 R_2 [1 + 2RT(\cos \epsilon - 1)]^N$. For small ϵ , Eq. (6) reduces to

$$\frac{4T_1 T_2 \sqrt{R_1 R_2}}{(1 - R_1 R_2)^2} \left[1 - \left(\frac{1}{2} + \frac{R_1 R_2}{1 - R_1 R_2} \right) NRT\epsilon^2 + \mathcal{O}(\epsilon^4) \right] \quad , \quad (7)$$

so for small ϵ the peak height depends linearly on shot noise $NRT = NT(1 - T)$ and quadratically on T , as noted above [22]. But when ϵ is not small, Eq. (6) tends to saturate in T for large bias (large N), as the fits to Fig. 3(a) show.

Equation (5) also leads to a formula for the broadening of the resonance peak as a function of detector bias and partitioning:

$$\text{FWHM} = \frac{\hbar}{t_{\text{tap}}} \arctan \frac{1}{2} \left[\frac{1}{\sqrt{Z}} - \sqrt{Z} \right] . \quad (8)$$

Equation (8) implies saturation of broadening before $T_{\text{eff}}(1 - T_{\text{eff}})$ reaches its maximum value, for large bias. Yet Fig. 3(b) indicates “anti-saturation” in T_{eff} : that is, the data do not level off in the middle of the range of T_{eff} but cluster upwards in the form of a triangle. This apparent inconsistency with our model may be understood as an artifact of the multiplicity of peaks. Each peak is enhanced by the tails of its neighbors, and this enhancement increases with the increased dephasing of the peaks. The enhancement does not significantly affect the apparent height of a peak, which is measured farthest from the neighboring peaks, but strongly affects apparent broadening. In addition, a Fabry-Perot resonance is equivalent to a Lorentzian only near the peak. Hence we have not applied Eq. (8) to Fig. 3(b) for the largest bias.

Additional support for our analysis of dephasing comes from measurements which we made on the same mesoscopic device, but with another setup at filling factor 3 and electron temperature of ~ 100 mK. These measurements checked the dependence of dephasing on the magnetic field at $B = 4.0$ T and $B = 4.3$ T, within the $3e^2/h$ conductance plateau. Since the $\nu = 2$ and $\nu = 3$ edge channels are separated by a cyclotron gap, we expect large channel separation and weaker dephasing, in accord with the small- ϵ limit of Eq. (5). For small ϵ , Eq. (8) implies a broadening in FWHM proportional to $NRT\epsilon^2$. Indeed, we found that the FWHM depended linearly on $IT_{\text{eff}}(1 - T_{\text{eff}})$ and that the slope of the line was some 40% higher at $B = 4.0$ T than at $B = 4.3$ T.

In summary, we have demonstrated controlled dephasing of a resonant tunneling device (a quantum dot) and showed how the dephasing depends on the detector current and partitioning. Controlled dephasing was realized in the integer quantum Hall regime, where we exploited the close proximity of edge channels to strongly entangle a small number of electrons.

Acknowledgments

We thank Yang Ji, Yunchul Chung, Michal Avinun and Izhar Neder for technical help and Florian Marquardt and Izhar Neder for helpful discussions. O. Zarchin acknowledges support from the Israeli Ministry of Science and Technology. This work was partly supported by the MINERVA foundation, the German Israeli foundation (GIF), the German Israeli project cooperation (DIP), and the Israeli Science foundation (ISF).

- [1] A. Einstein, B. Podolsky and N. Rosen, *Phys. Rev.* **47**, 777, (1935).
- [2] E. Schrödinger, *Naturwiss.* **48**, 807, 823 and 844 (1935); *Proc. Am. Phil. Soc.* **124**, 323 (1980).
- [3] J. S. Bell, *Physics* **1**, 195 (1964).
- [4] S. Weisner, *Sigact News* **15**, 78 (1983); A. K. Ekert, *Phys. Rev. Lett.* **67**, 661 (1991).
- [5] C. H. Bennett et al., *Phys. Rev. Lett.* **70**, 1895 (1993).
- [6] R. Jozsa and B. Schumacher, *J. Mod. Optics* **41**, 2343 (1994); B. Schumacher, *Phys. Rev.* **A51**, 2738 (1995).
- [7] See *Introduction to Quantum Computation and Information*; eds. H.-K. Lo, S. Popescu, and T. P. Spiller (Singapore: World Scientific), 1998.
- [8] For a brief review see D. Rohrlich, *Op. Spec.* **99**, 503 (2005).
- [9] A. Yacoby et al., *Phys. Rev. Lett.* **74**, 4047 (1995).
- [10] R. Schuster et al., *Nature* **385** 417 (1997).
- [11] D. Sprinzak et al., *Phys. Rev. Lett.* **84**, 5820 (2000).
- [12] Y. Ji et al., *Nature* **422**, 415 (2003).
- [13] M. Field et al., *Phys. Rev. Lett.* **70**, 1311 (1993).
- [14] E. Buks et al., *Nature* **391**, 871 (1998).
- [15] R. P. Feynman, R. B. Leighton and M. Sands, *The Feynman Lectures on Physics, Vol. III* (Reading, MA: Addison–Wesley Pub. Co.), 1965, p. 1-9. See also Y. Aharonov and D. Rohrlich, *Quantum Paradoxes: Quantum Mechanics for the Perplexed* (Weinheim: Wiley-VCH), 2005, Sect. 18.1.
- [16] A. Stern, Y. Aharonov and Y. Imry, *Phys. Rev.* **A41**, 3436 (1990).
- [17] For a review see M. Reznikov et al., *Superlattices and Microstructures* **23**, 901 (1998). The

term “shot noise” is often identified with the factor $NT(1 - T)$.

- [18] We rewrite $e^{i \sum_{k=j'N}^{jN} \epsilon_k}$ as $\prod_{k=j'N}^{jN} e^{i\epsilon_k}$, and the expectation value of $e^{i\epsilon_k}$ is $R + e^{i\epsilon}T$.
- [19] J. H. Davies, J. C. Egues and J. W. Wilkins, *Phys. Rev.* **B52**, 11259 (1995). For ϵ small, we have $|R + e^{i\epsilon}T|^N \approx e^{-NRT\epsilon^2/2} = e^{-NT(1-T)\epsilon^2/2}$.
- [20] R. de-Picciotto et al., *Nature* **389**, 162 (1997); M. Reznikov et al., *Nature* **399**, 238 (1999).
- [21] By applying a DC bias to the tunneling current, we shift the energies of the electrons at resonance by a known amount. The shift shows up as a shift in the Coulomb blockade peaks. Comparing this calibrated shift with the energy scale defined by the plunger gate potential, we extract a leveraging factor with which we convert the width in *plunger gate potential* of a Coulomb blockade peak into width in *electron energy*.
- [22] We recognize the factor $1/2 + R_1R_2/(1 - R_1R_2)$ in Eq. (7) as the average number of laps of a tunneling electron, as calculated.

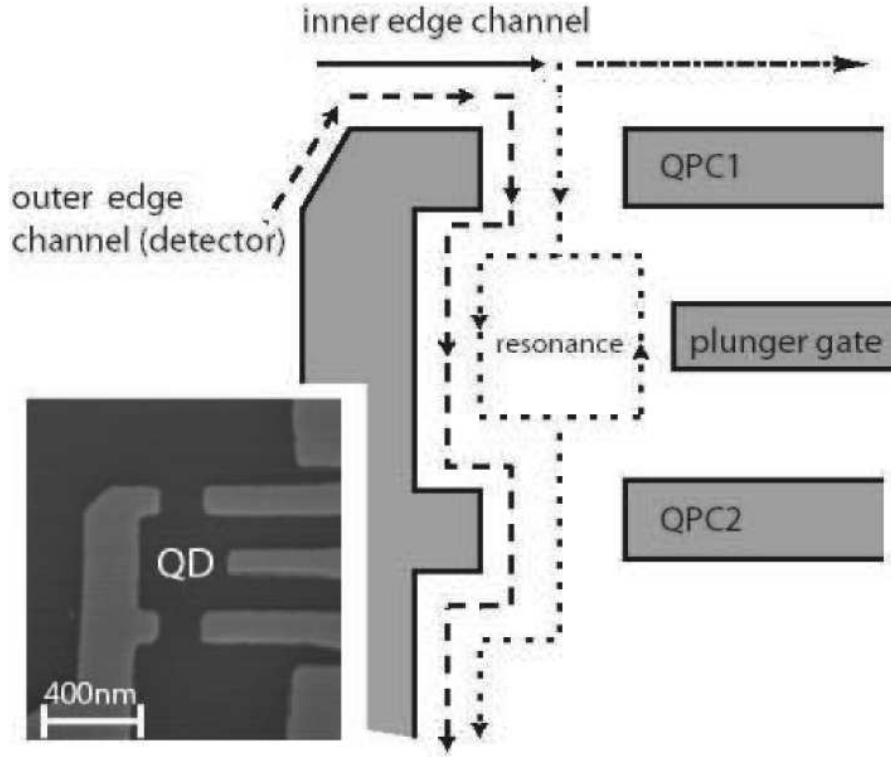


FIG. 1: Diagram of the quantum dot, defined by biased metallic electrodes (two QPCs and a “plunger gate”) over a high-mobility two-dimensional electron gas (2DEG) of density $2 \times 10^{11}/\text{cm}^2$ embedded in a GaAs-AlGaAs heterojunction. At magnetic field 5-7 T the 2DEG is at the filling-factor 2 plateau. Two quantum Hall edge channels enter from above. The inner current channel crosses via resonant tunneling and the outer current, partitioned at a prior quantum point contact, serves as a detector. Inset: SEM micrograph of a similar dot, $0.4 \mu\text{m}$ wide inside.

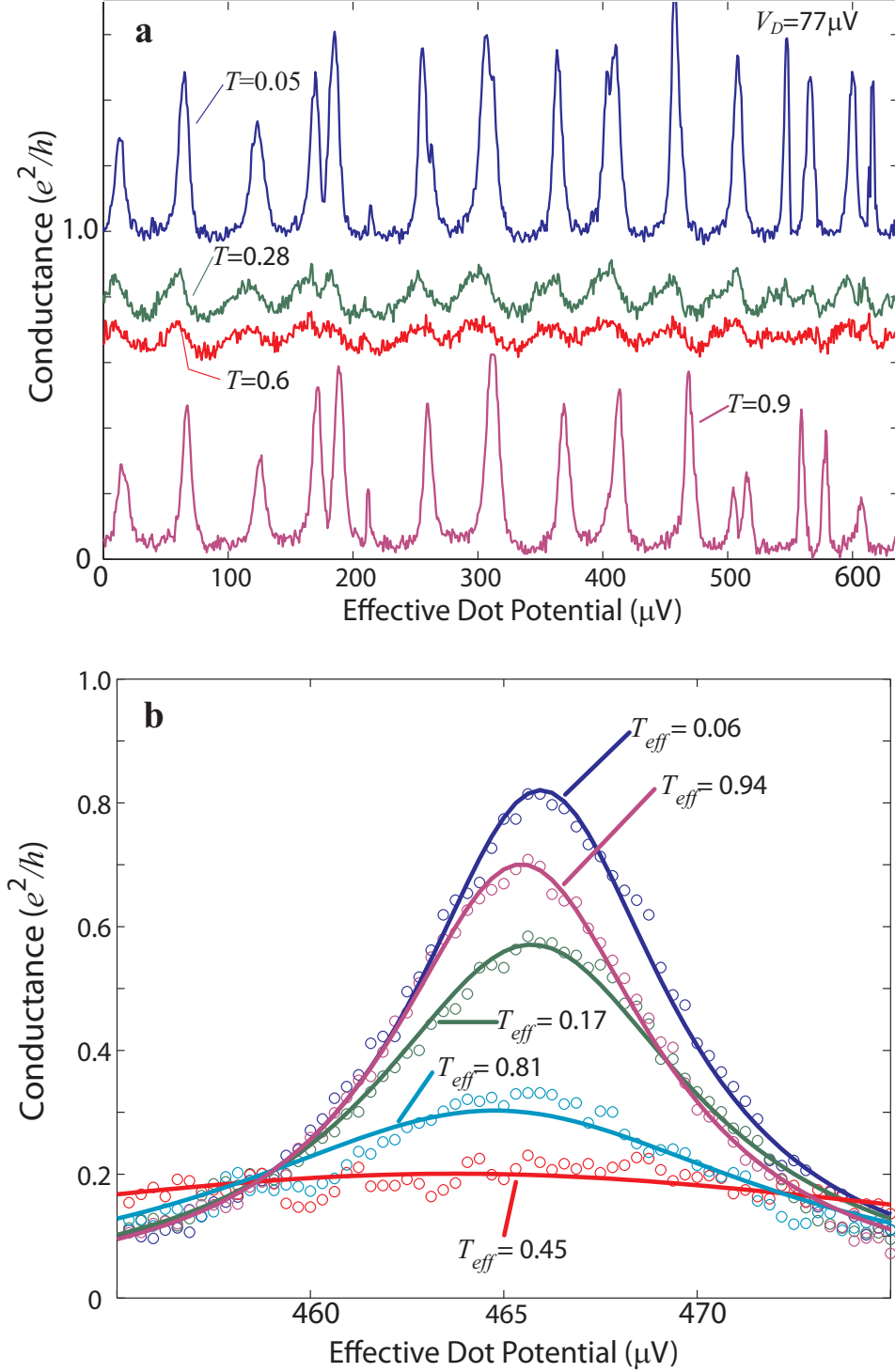


FIG. 2: Dephasing of resonance peaks at filling factor 2, with $77\ \mu\text{V}$ DC bias on the detector. (a) The horizontal axis shows the potential on the plunger gate, normalized to effective dot potential. The vertical axis shows the resonant conductance through the inner channel (shifted), ranging from $T \approx 0$ (top trace) to $T \approx 1$ (bottom trace). (b) Dephasing of a typical resonance peak. The vertical axis shows the resonant conductance. Circles are experimental results while lines are Lorentzian fits.

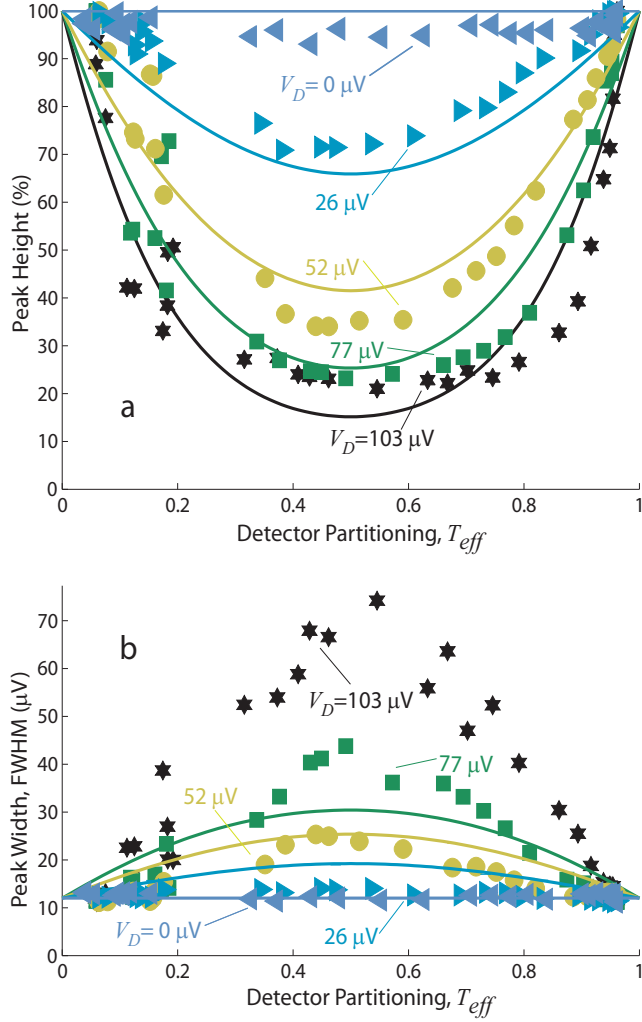


FIG. 3: Plots of (a) quenching (as percentage of the original peak height) and (b) peak width FWHM, as functions of the effective detector transmission T_{eff} and detector bias. Symbols represent experimental results. In (a), continuous lines are fits to Eq. (6), with $\epsilon = 0.45\pi$ and N ranging from 4 for detector bias $\pm 103 \mu\text{V}$ to 0 for detector bias $0 \mu\text{V}$. In (b), continuous lines are fits to Eq. (8) (with the same N and ϵ) for same detector bias.